01 Jun 2005

Liquid Saturation and Gas-Liquid Distribution in Multiphase Monolithic Reactors

Tobias Bauer

Shaibal Roy

Ruediger Lange

Muthanna H. Al-Dahhan
Missouri University of Science and Technology, aldahhanm@mst.edu

Recommended Citation

T. Bauer et al., "Liquid Saturation and Gas-Liquid Distribution in Multiphase Monolithic Reactors," *Chemical Engineering Science*, vol. 60, no. 11, pp. 3101 - 3106, Elsevier, Jun 2005.
The definitive version is available at https://doi.org/10.1016/j.ces.2004.12.041

Chemical Engineering Science 60 (2005) 3101–3106

Chemical Engineering Science

www.elsevier.com/locate/ces

Liquid saturation and gas–liquid distribution in multiphase monolithic reactors

Tobias Bauer[a], Shaibal Roy[b], Ruediger Lange[a], Muthanna Al-Dahhan[b,]*

[a]*Department of Chemical Engineering, Dresden University of Technology, Muenchner Platz 3, 01062 Dresden, Germany*
[b]*Chemical Reaction Engineering Laboratory (CREL), Department of Chemical Engineering, Washington University in St. Louis, One Brookings Drive, Campus Box 1198, St. Louis, MO 63130 4899, USA*

Received 27 April 2004; received in revised form 12 November 2004; accepted 22 December 2004

Abstract

The monolith bed is one of the promising catalytic reactors for a number of chemical gas–liquid–solid processes. In the present work, liquid saturations for five different monoliths have been investigated experimentally in a cold-flow unit with a reactor diameter of 5.0 cm. The influences of gas and liquid flow rates and of the direction of two-phase flow on liquid saturation were examined. The results indicate that the direction of flow has no significant influence on liquid saturation for proper gas–liquid distribution. The experimental results are in good agreement with predictions of the drift flux model using the distribution parameter proposed by Ishii (ANL Report ANL-77-47, 1977) along with the assumption of zero drift velocity.

In preliminary experiments, gamma-ray computed tomography (CT) has been successfully applied to measure time-averaged liquid distribution over the monolith cross-section in a selected condition. The employment of a nozzle-type distributor provides an almost uniform liquid distribution over the monolith substrate. It is demonstrated that CT is a viable technique for studying two-phase flow in laboratory-scale monolith reactors.

Keywords: Monolith; Multiphase flow; Hydrodynamics; Liquid saturation; Flow distribution; Computed tomography

1. Introduction

For the execution of three-phase gas–liquid–solid reactions encountered in different industries, various types of multiphase flow reactors have been used such as stirred tank slurry reactors, slurry bubble columns and packed bed reactors. Recently, research has led to the utilization of structured packing instead of slurry or randomly packed reactors. One of the promising structured beds is the so-called monolith. Monoliths and other structured packings have been used successfully for abatement of car emissions and in mass transfer operations such as distillation and absorption (Cybulski and Moulijn, 1998). A number of investigations have shown favorable performance for selected gas–liquid–solid reactions in laboratory and pilot-scale studies (Roy et al., 2004a). In general, the hydrodynamics are important criteria for proper selection of multiphase reactors (Krishna and Sie, 1994) and for their design and scale-up. Thus, a detailed understanding of the hydrodynamics of monolithic reactors and their influencing parameters such as superficial velocities, reactor pressure, channel structure, direction of flow, gas–liquid distribution, etc. is needed.

The reported investigations on various aspects of the monolithic reactors have been performed using single capillary experiments and cold-flow laboratory-scale set-ups. In general, air–water two-phase flow in capillaries has been used and extensively studied (Zhao and Bi, 2001; Simmons et al., 2003). Little work has been reported so far on liquid holdup or saturation measurements in monolith reactors for co-current flow operation. Grolman et al. (1996)

---

* Corresponding author. Tel.: +1 314 935 7187; fax: +1 314 935 7211.
E-mail address: muthanna@che.wustl.edu (M. Al-Dahhan).

0009-2509/$ - see front matter © 2005 Elsevier Ltd. All rights reserved.
doi:10.1016/j.ces.2004.12.041

and Heiszwolf et al. (2001) investigated liquid saturation experimentally by means of a weighing method in a downflow monolith reactor. More recently, Vandu et al. (2004) have measured gas holdup in an upflow monolith loop reactor configuration. However, most of the published studies are limited to monolith properties and do not highlight the impact of structure or direction of flow.

One of the major challenges in the design and operation of monolith reactors is the prevention of gas–liquid maldistribution, which leads to underutilization of the catalyst bed. Nowadays, sophisticated techniques such as computed tomography (CT) and magnetic resonance imaging have been used to study gas–liquid distribution in monolith reactors. Mewes et al. (1999) studied gas–liquid distribution over the reactor cross-section in monoliths using capacitance tomography. The authors demonstrated the influence of different liquid flow rates at zero gas flow rate on liquid distribution. More recently, Mantle et al. (2002) and Gladden et al. (2003) have used magnetic resonance imaging (MRI) to visualize slug flow and slug size distribution in monolith structures. Unfortunately, results have been reported only for a narrow range of flow conditions. Heibel et al. (2003) have focused on flow distribution in film-flow monolithic reactors using the liquid collection method and MRI.

In the present study, external liquid saturation was investigated experimentally using the weighing method. Experiments were conducted at atmospheric pressure over a range of industrially relevant gas and liquid velocities and for five different monolith structures. Furthermore, the applicability of gamma-ray CT for the measurement of two-phase flow distribution in a monolithic reactor was demonstrated for a selected condition.

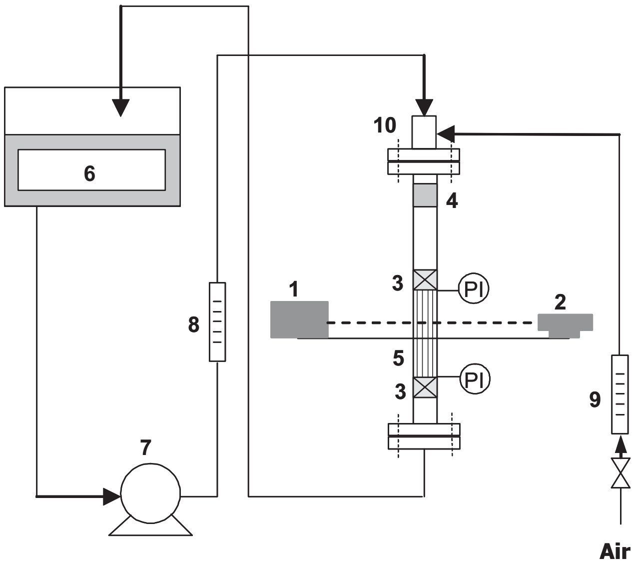

Fig. 1. Schematic diagram of the cold-flow unit and CREL computed tomography (CT) facility with monolith reactor inside for operation in co-current downflow: 1 source, 2 detector, 3 gate valve, 4 distributor, 5 monolith, 6 liquid reservoir tank, 7 liquid pump, 8 liquid rotameter, 9 gas rotameter, 10 reactor.

Table 1
Geometrical specifications of the monoliths

Monolith	100-25	300-5	400-4	400-7	600-4
Cell density (cells/cm^2)	15.5	46.5	62.0	62.0	93.0
Diameter (cm)	5.0	5.0	4.9	5.0	5.0
Length (cm)	15.2	15.2	14.6	15.2	15.2
OFA (%)	56	83	85	75	82
GSA (m^2/m^3)	1175	2480	2902	2406	3476
Hydraulic diameter (mm)	1.91	1.34	1.17	1.1	0.94
Wall thickness (mm)	0.64	0.13	0.1	0.2	0.1

2. Experimental work

An experimental set-up (Fig. 1) has been assembled which can be operated in co-current upflow and downflow modes of operation over a range of liquid and gas velocities. Liquid from the feed tank was pumped (Teel pump, model 1V275-0397) into the column through a rotameter (Omega Inc., model FL-75) and adjusted by a valve. Air from the in-house utility line was fed co-currently at the bottom or at the top of the column. The gas flow rate was measured and adjusted by a rotameter (Dwyer Instruments Inc., model Rate Master).

The reactor was constructed of clear PVC pipe (Sch 40) with a nominal diameter of 5.0 cm. For operation in upflow mode, gas was distributed through a foam ceramic distributor (characterized by 8 pores cm, from Porvair) located underneath the bottom of the monolith. For sufficiently high liquid velocities, a turbulent gas–liquid froth was formed above the distributor unit. In downflow operation, the liquid was distributed over the monolith channels using a commercial spray nozzle. For sufficiently high liquid and gas velocities, a thick layer of foam was produced over the packing. The reactor section was packed with a block of cordierite monolith (provided by Corning) with a diameter of 5.0 cm and a length of 15.0 cm. The gas and liquid phases flew together out of the reactor to the feed tank where the gas was vented while the liquid was re-circulated to the reactor. The specifications of the monoliths used in this study are listed in Table 1. External liquid saturation was measured by simultaneously shutting off the entrance and exit valves of the monolith bed. This reactor section was dismantled and its weight was measured. Liquid saturation was calculated by subtracting the weight of the reactor including the liquid saturated monolith substrate from the total weight of the dismantled section.

For selected conditions, gamma-ray CT scans were performed at the middle height of the monolith bed to characterize the flow distribution. A schematic diagram of the system is illustrated in Fig. 4. The newly developed scanner (Roy et al., 2004b) consists of an encapsulated $\sim$70 mCi Cs^{137} source as well as of an array of nine NaI detectors located opposite to the source. Both the source and the detectors are mounted on a plate, which can be rotated around the axis of the monolithic reactor by a stepping motor. The CT scans were obtained by scanning 360° around the reactor with a total scanning time of about 5 h. The beam attenuation is measured along a number of beam paths through the monolithic reactor, which originate from different angles. The density distribution image is reconstructed by using the Estimation-Maximization algorithm (Kumar and Dudukovic, 1997). The final liquid saturation images are obtained from the attenuation data using the procedure developed by Chen et al. (2001) for packed bed reactors.

3. Results

3.1. Liquid saturation

Total liquid saturation β_L is defined as the ratio of the liquid volume present in the monolith bed to the volume of the bed voidage, Eq. (1). The monolith bed voidage is also called open frontal area (OFA) and represents that part of the total substrate cross-section area which is available for the flow of gas and liquid. The OFA is frequently expressed as a percentage of the total substrate cross-section and sometimes also called the substrate void fraction.

$$\beta_L = V_L/(V_L + V_G), \tag{1}$$

$$\beta_L = V_L/(V_{\text{monolith}}\,\text{OFA}), \tag{2}$$

$$\beta_L + \beta_G = 1. \tag{3}$$

Liquid saturation was experimentally investigated for liquid superficial velocities in the range of 3.0 to 17.0 cm/s and gas superficial velocities in the range of 3.0 to 21.0 cm/s. Flow maps (Simmons et al., 2003) indicate that the reactor was operated in the slug flow (Taylor flow) regime over the whole range of gas and liquid velocities.

Fig. 2 shows the influence of gas and liquid flow rates on liquid saturation in downflow mode of operation. For a constant liquid flow rate, the liquid saturation decreases with increasing gas flow rate. Similar behavior was observed for all experiments in downflow mode of operation. For reactors operating in upflow mode and at a low liquid superficial velocity (3.0 cm/s), the liquid saturation differs significantly from that in downflow mode. The liquid saturation for these experiments was remarkably higher. The discrepancy was between 75% and 92% and was observed for all five monoliths used. The deviation could be attributed to the type of the distributor used for upflow operation, which in this case was a foam type as mentioned earlier. In the case of low liquid velocity (3.0 cm/s), the gas distribution over the cross-section at the bottom of the monolith bed was visually observed to be poor. At this condition the path of rising gas bubbles was localized and not evenly distributed throughout the whole reactor cross-section. For higher liquid superficial velocities of 9.0 to 17 cm/s visual observations have shown a thick and chaotic mixed layer underneath the monolith. Fig. 3 shows a parity plot of the measured liquid saturation for the monolithic reactor operated in upflow mode versus liquid saturation in downflow mode. As depicted in the figure, the direction of flow has no significant influence on liquid saturation if gas and liquid distributions are of the same quality. The figure indicates that for superficial liquid velocities in the range of 9.0 to 21.0 cm/s the deviation in liquid

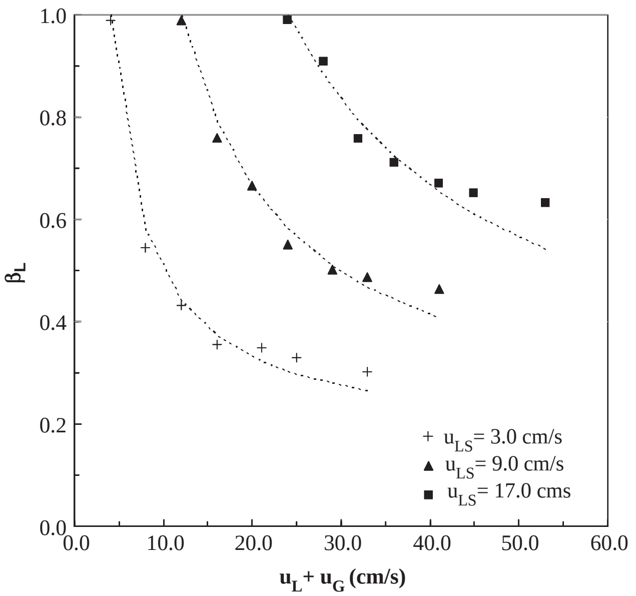

Fig. 2. Liquid saturation for three different liquid velocities and the predictions of Eq. (8) (dashed lines) for a monolith of a channel density of 62 channels/cm^2 operated in downflow mode.

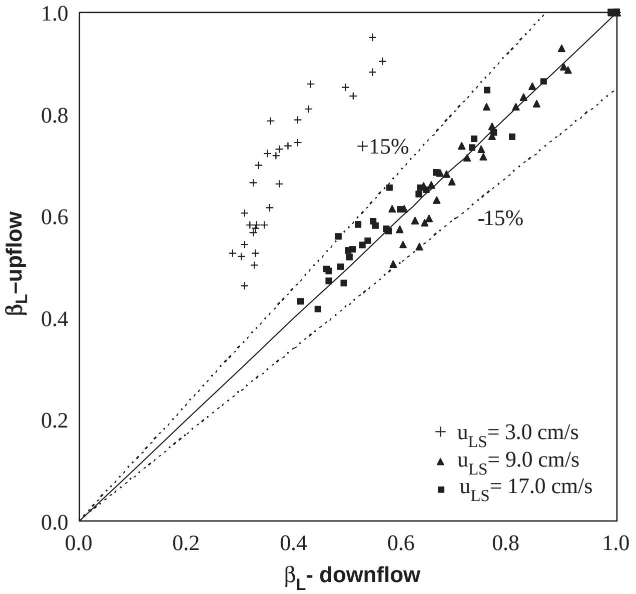

Fig. 3. Parity plot of liquid saturation for five monoliths (Table 1) operated in upflow and downflow modes for superficial liquid velocities between 3.0 and 17.0 cm/s and superficial gas velocities between 3.0 and 21.0 cm/s.

saturation in upflow and downflow modes is within ±15%. The remarkable discrepancy for a low liquid velocity of 3.0 cm/s is due to the gas–liquid maldistribution, which arises in upflow mode of operation as mentioned above. The structure of a monolith bed consists of an array of small parallel channels, which can be seen as single square capillaries. For homogeneous gas–liquid distribution over the monolith bed, every channel should have the same liquid saturation. Therefore, one would predict liquid saturation using correlations that are available for single capillaries. Simmons et al. (2003) have reported that overall shapes of flow maps are relatively similar between round and square capillaries. Moreover, the slug flow (Taylor flow) regime was very similar in both location and shape. This underlines the application of correlations derived for round capillaries to model liquid saturation within monolith beds. A general approach to characterize gas–liquid flow in tubes is given by the drift flux model (Wallis, 1969). Eq. (4) gives the relationship between gas velocity and the mixture volumetric flux ($u_L + u_G$).

$$v_G = u_G/\beta_G = C_0(u_L + u_G) + U_G, \tag{4}$$

where β_G is the gas saturation, C_0 is the distribution parameter and U_G is the drift velocity. For operation in the slug flow (Taylor flow) regime of tubes with larger diameter, Ishii (1977) proposed Eqs. (5) and (6) to describe the distribution parameter and drift velocity, respectively.

$$C_0 = 1.2 - 0.2\sqrt{\rho_G/\rho_L}, \tag{5}$$

$$U_G = 0.35\sqrt{\Delta\rho g d/\rho_L}, \tag{6}$$

For small tube diameter with $d < 5$ mm the drift velocity becomes zero (Zhao and Bi, 2001). Therefore, the drift velocity was ignored in the drift flux model given by Eq. (4).

The combination of Eqs. (4) and (5) yields the following expression for liquid saturation:

$$\beta_L = 1 - [(1.2 - 0.2\sqrt{\rho_G/\rho_L})^{-1} u_G/(u_G + u_L)]. \tag{7}$$

For air/water two-phase flow system at atmospheric pressure and room ambient temperature, Eq. (7) becomes as follows:

$$\beta_L = 1 - [0.838 u_G/(u_G + u_L)]. \tag{8}$$

Fig. 4 compares this correlation (Eq. (8)) with experimental data obtained in this work. The predicted values are within ±20% of the measured values. The correlation underpredicts liquid saturation for the low superficial liquid velocity (3.0 cm/s) in upflow mode of operation due to gas–liquid maldistribution as explained earlier. These data for upflow mode of operation is not depicted in the figure.

3.2. Gas–liquid distribution using computed tomography

The monolith bed voidage of dry monolith substrate was first measured experimentally using the CT technique. It was found that the CT unit used measures the monolith bed porosity within 2–3% deviation from the value provided by the manufacturer (Corning Inc.).

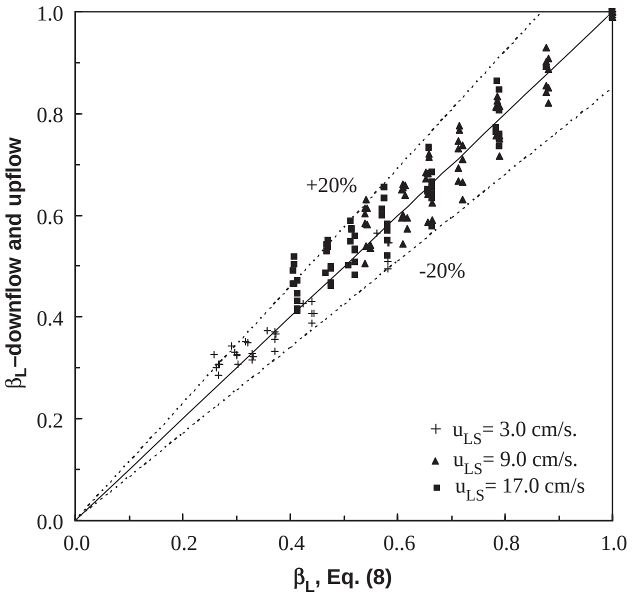

Fig. 4. Parity plot of liquid saturation versus prediction by Eq. (8) for upflow and downflow mode of operation for superficial liquid velocities between 3.0 and 17.0 cm/s and superficial gas velocities between 3.0 and 21.0 cm/s.

Fig. 5a shows a typical time average cross-sectional distribution of the liquid saturation in a monolith bed at atmospheric pressure operated in downflow mode of operation. The figure indicates that the cross-sectional liquid saturation distribution in a monolith reactor is close to uniform in the conditions listed in Fig. 5.

Fig. 5b illustrates the azimuthally averaged radial liquid saturation profile. This radial profile also highlights the fact that for the gas and liquid superficial velocities used, the nozzle-type distributor gives almost uniform distribution. This finding is in good accordance with previews results form Heibel et al. (2003). The authors reported the achievement of very uniform distribution if applying a nozzle-type distributor. Such assessment of the quality of liquid distribution is necessary to guarantee maximum benefit from the monolith reactors. The decrease in liquid saturation close to the reactor wall is attributed to the influence of the Teflon packing used to hold the substrate in place. The external liquid saturation obtained from the analysis of the azimuthally averaged radial liquid saturation profile is about 71%. However, the calculated liquid saturation from Eq. (8) for the gas and liquid velocities used is about 73%. For this particular condition the experimental result obtained from the CT scan is in reasonable agreement with the prediction of the correlation (Eq. (8)). This further indicates uniform distribution of the liquid phase over the reactor cross-section, since correlations (7) and (8) have been developed based on uniform distribution of the phases over the monolith bed.

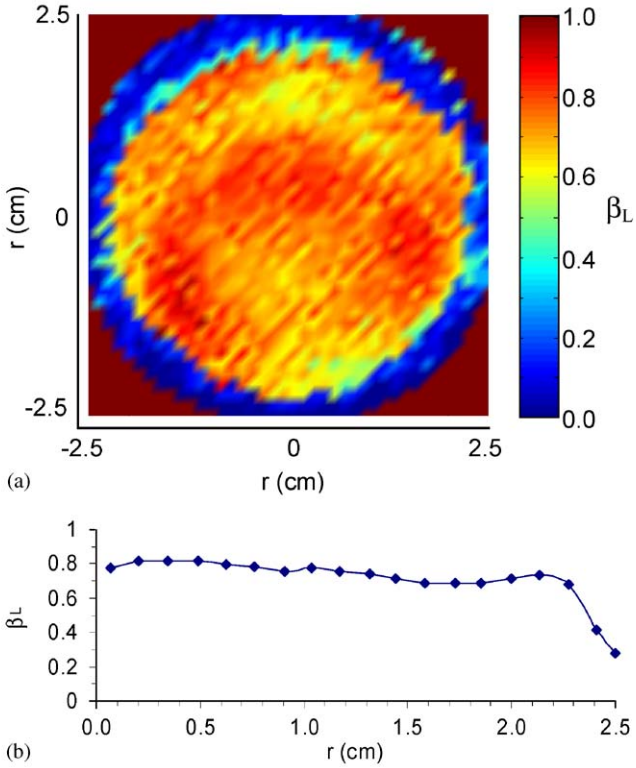

Fig. 5. Liquid saturation β_L for a monolith bed of a cell density of 62 cells/cm^2 and OFA of 75% at $u_{LS} = 20.0$ cm/s and $u_{GS} = 10.0$ cm/s in downflow mode of operation (a) time-averaged cross-sectional liquid saturation distribution (b) azimuthally averaged radial liquid saturation profile.

4. Conclusion and future work

A study was conducted to evaluate liquid saturation and flow distribution in different monolith bed structures. It was found that for sufficiently high superficial liquid flow rates (above 9.0 cm/s) the direction of flow has no significant influence on liquid saturation. The liquid saturation was predicted by the correlation proposed by Ishii (1977) within ±20% for the slug flow regime and zero slip velocity.

In preliminary experiments, computed tomography (CT) was applied to determine cross-sectional liquid saturation distribution and a radial liquid saturation profile in the monolith bed in a selected condition. The cross-sectional averaged liquid saturation obtained by CT is in agreement with the prediction of the mentioned correlation. First experiments have proven that gamma-ray CT is a viable technique for studying two-phase flow distribution in laboratory-scale monolithic reactors. Since gas–liquid distribution is an important issue for the performance of multiphase monolithic reactors it needs further investigation for a broader range of conditions. A more detailed study on the impact of monolith geometry and direction of flow on liquid saturation and gas–liquid distribution is currently underway.

Notation

C_0	distribution parameter
d	capillary diameter (mm)
g	gravity (m/s^2)
GSA	geometric surface are (m^2/m^3)
OFA	open frontal area
u_G	gas velocity within a channel (m/s)
u_{GS}	superficial gas velocity (m/s)
u_L	liquid velocity within a channel (m/s)
u_{LS}	superficial liquid velocity (m/s)
U_G	drift velocity (m/s)
V_G	gas volume (m^3)
V_L	liquid volume (m^3)
V_{monolith}	monolith bed volume (m^3)

Greek letters

$\Delta\rho$	density difference (kg/m^3)
β_G	gas saturation
β_L	liquid saturation
ρ_G	gas density (kg/m^3)
ρ_L	liquid density (kg/m^3)

Indices

G	gas
L	liquid
S	superficial

Acknowledgements

The authors would like to acknowledge Air Products and Chemicals for donating the experimental set-up, Corning Inc. for providing the different sets of monolith substrates used in this research and Bayer and the Chemical Reaction Engineering Laboratory (CREL) for partial financial support.

References

Chen, J., Rados, N., Al-Dahhan, M., Dudukovic, M.P., Nguyen, D., Parimi, K., 2001. Particle motion in packed/ebullated beds by CT and CARPT. A.I.Ch.E. Journal 47, 994–1004.

Cybulski, A., Moulijn, J.A., 1998. Structured Catalysts and Reactors. Marcel Dekker Inc., New York.

Gladden, L.F., Lim, M.H.M., Mantle, M.D., Sederman, A.J., Stitt, E.H., 2003. MRI visualisation of two-phase flow in structured supports and trickle-bed reactors. Catalysis Today 79–80, 203–210.

Grolman, E., Edvinsson, R.K., Stankiewicz, A., Moulijn, J.A., 1996. Hydrodynamic instabilities in gas-liquid monolithic reactors. Proceedings of the American Society of Mechanical Engineers. Heat Transfer Division 334 (3), 171–178.

Heibel, A.K., Vergeldf, F.J., van As, H., Kapteijn, F., Moulijn, J., Boger, T., 2003. Gas and liquid distribution in the monolith film flow reactor. A.I.Ch.E. Journal 49 (12), 3007–3017.

Heiszwolf, J.J., Engelvaart, L.G., van den Eijnden, M.T., Kreutzer, M., Kapteijn, F., Moulijn, J.A., 2001. Hydrodynamic aspects of the monolith loop reactor. Chemical Engineering Science 56 (3), 805–812.

Ishii, M., 1977. One-dimensional drift-flux model and constitutive equations for relative motions between phases in various two-phase flow regimes. ANL Report ANL-77-47.

Krishna, R., Sie, S.T., 1994. Strategies for multiphase reactor selection. Chemical Engineering Science 49, 4029–4065.

Kumar, S.B., Dudukovic, M.P., 1997. Computer assisted gamma and X-ray tomography: applications to multiphase flow systems. Non-Invasive Monitoring of Multiphase Flows 47-103.

Mantle, M.D., Sederman, A.J., Gladden, L.F., Raymahasay, S., Winterbottom, J.M., Stitt, E.H., 2002. Dynamic MRI visualization of two-phase flow in a ceramic monolith. A.I.Ch.E Journal 48 (4), 909–912.

Mewes, D., Loser, T., Millies, M., 1999. Modelling of two-phase flow in packings and monoliths. Chemical Engineering Science 54 (21), 4729–4747.

Roy, S., Bauer, T., Lehner, P., Turek, T., Al-Dahhan, M., 2004a. Monoliths as multiphase reactors: a review. A.I.Ch.E. Journal 50 (11), 2918–2938.

Roy, S., Kemoun, A., Al-Dahhan, M.A., Dudukovic, M.P., Skourlis, T.B., Dautzenberg, F.M., 2004b. Countercurrent flow distribution in structured packing via computed tomography. Chemical Engineering and Processing 44 (1), 59–69.

Simmons, M.J., Wong, D.C.Y., Travers, P.J., Rothwell, J.S., 2003. Bubble behavior in three phase capillary microreactors. International Journal of Chemical Reactor Engineering 1, A30.

Vandu, C.O., Ellenberger, J., Krishna, R., 2004. Hydrodynamics and mass transfer in an upflow monolith loop reactor. Chemical Engineering and Processing 44 (3), 363–374.

Wallis, G.B., 1969. One Dimensional Two-Phase Flow. Mc-Graw Hill, New York.

Zhao, T.S., Bi, Q.C., 2001. Pressure drop characteristics of gas–liquid two-phase flow in vertical miniature triangular channels. International Journal of Heat and Mass Transfer 44 (13), 2523–2534.